European Radiology (2019) 29:4538–4543
https://doi.org/10.1007/s00330-019-5998-1

CHEST

Optimal beam quality for chest flat panel detector system: realistic phantom study

Chie Kuwahara[1] · Takatoshi Aoki[1] · Nobuhiro Oda[2] · Jun Kawabata[1] · Koichiro Sugimoto[1] · Michiko Kobayashi[1] · Masami Fujii[1] · Yukunori Korogi[1]

Received: 28 July 2018 / Revised: 9 December 2018 / Accepted: 4 January 2019 / Published online: 8 February 2019

Abstract

Objective To investigate optimal beam quality for chest flat panel detector (FPD) system by semi-quantitatively assessment using a realistic lung phantom.

Materials and methods Chest FPD radiographs were obtained on a realistic lung phantom with simulated lung opacities using various X-ray tube voltage levels (90–140 kV) with/without copper filter. Entrance skin dose was set to maintain identical for all images (0.1 mGy). Three chest radiologists unaware of the exposure settings independently evaluated the image quality of each simulated opacity and normal structure using a 5-point scale (+ 2: clearly superior to the standard; + 1: slightly superior to the standard; 0: equal to the standard; − 1: slightly inferior to the standard; − 2: clearly inferior to the standard). The traditional FPD image obtained at a tube voltage of 120 kV was used as the standard. The scores of image quality were statistically compared using the Wilcoxon rank test with Bonferroni correction.

Results FPD images using 90-kV shot with copper filter were superior to the traditional 120-kV shot without filter with respect to the visibility of vertebra, pulmonary vessels, and nodules overlapping diaphragm and heart ($p < 0.05$). There was no significant difference with respect to the visibility of all other simulated lung opacities (lung nodules except for overlying diaphragm/heart and honeycomb opacity) between each tube voltage level with/without copper filter and the traditional 120-kV shot without filter.

Conclusion Image quality of FPD images using 90 kV with copper filtration is superior to that using standard tube voltage when dose is identical.

Key Points

- *FPD image quality using 90 kV with filter is superior to that using traditional beam.*
- *Ninety-kilovolt shot with copper filter may be suitable for chest FPD image.*
- *Clinical study dealing with chest FPD beam optimization would be warranted.*

Keywords Digital radiography · Chest radiography · Physics · Dose · Image quality

Abbreviations

CNRs	Contrast-to-noise ratios
CR	Computed radiography
DR	Digital radiography
ESD	Entrance skin dose
FPD	Flat panel detector
ICC	Intraclass correlation coefficients
PMMA	Polymethyl methacrylate

Introduction

Because of recent advances in medical devices, digital radiography (DR), such as computed radiography (CR) and flat panel detector (FPD), has replaced analog technology. Owing to the limited dynamic range of conventional film chest radiographs, the exposure parameter is inevitably determined for displaying large variability in radiopacity of organs in the thoracic cavity in the same plane. In contrast, DR has the advantage of optimization of image contrast among various organs due to wide

✉ Takatoshi Aoki
a-taka@med.uoeh-u.ac.jp

[1] Department of Radiology, University of Occupational and Environmental Health, 1-1 Iseigaoka, Yahatanishi-ku, Kitakyushu 807-8555, Japan

[2] Department of Radiological Technology, Kyoto College of Medical Science, Kyoto, Japan

dynamic range and image processing, which allows overexposure with no effect on image quality [1, 2]. Therefore, it is necessary to determine optimal beam quality for DR systems.

According to the American College of Radiology standards for the performance of chest radiography, a high-kilovoltage technique (120 to 150 kV) is recommended for a posteroanterior chest radiograph in adults [3]. In Japan, chest DR is performed with a tube voltage of 120.9 ± 8.0 kV (total filtration, 3.6 ± 1.5-mm Al equivalent, without copper filter at most institutions), and the mean skin dose of chest radiograph showed an increasing tendency (0.21 mGy in 2001 and 0.28 mGy in 2014) [4, 5]. On the other hand, some previous studies reported that the image contrast of chest CR at a tube voltage of 90–100 kV was identical to that using a high tube voltage [6, 7] and others reported an improved signal-to-noise ratio with DR systems when images were acquired with lower voltage [8–10]. Further optimization of DR systems could possibly reduce the dose.

FPD system is becoming the mainstream of chest radiography due to excellent image quality and lower radiation exposure. Although there is a lot of room for improvement in the X-ray spectrum of FPD, there were no studies for evaluating optimal beam quality for chest FPD system by qualitative assessment using a realistic lung phantom.

The purpose of this study was to qualitatively investigate how beam optimization contributes to the improvement of image quality using a realistic lung phantom.

Materials and methods

Radiographic technique

An X-ray high-voltage generator (RADIOTEX, Shimadzu) with an X-ray tube having a 0.6 × 1.2-mm focal size (P18DE-811, Shimadzu) was used. A moving grid having a 10:1 ratio (40 lines/cm) was used for all radiographic exposures in this study. All images were obtained by a cesium iodide-amorphous silicon indirect FPD unit (CALNEO Smart C47, Fuji Film) using automatic image processing mode. The size of the detector area of the flat panel unit was 35 × 43 cm (matrix size, 2373 × 2880; gray level, 12 bits; pixel size, 0.15 mm).

Lung phantom

A commercially available realistic chest phantom (N-1, Kyoto Kagaku) was used in this study [11–13]. The phantom consisted of an accurate life-size anatomical model of a male thorax with soft tissue substitute materials made of polyurethane resin composites and synthetic bones made of epoxy resin with X-ray absorption rates close to those of human tissue. The space between the pulmonary vessels in the thoracic cavity consisted of air. The phantom measured 43 × 40 × 48 cm in dimension with a chest girth of 94 cm. Ten simulated nodules and one simulated honeycomb opacity were enclosed in the lung (Fig. 1). Simulated nodules were 10 mm in diameter with spherical shapes and their attenuation values were + 30, − 375, and − 620 HU, corresponding to the solid nodule, subsolid nodule, and ground-glass nodule on CT.

FPD image variables

First, in order to determine beam qualities to be compared, we investigated the contrast-to-noise ratios (CNRs) of simulated nodules on the FPD image using polymethyl methacrylate (PMMA) plates phantom inserted three different CT number nodules (diameter 10 mm, CT number + 30, − 375, − 620). The results showed that the CNRs of all three simulated nodules on the FPD images using 80–100-kV shot with copper filter were superior to those using 120–140-kV shot without filter (Fig. 2). Based on this result, chest FPD radiographs were obtained on a lung phantom with simulated lung opacities using various X-ray tube voltage levels with or without copper filter: (1) 90 kV with 0.2-mm filter, 8.8 mAs; (2) 90 kV with 0.15-mm filter, 7.1 mAs; (3) 100 kV with 0.2-mm filter, 6.4 mAs; (4) 100 kV with 0.1-mm filter, 4.5 mAs; (5) 100 kV without filter, 2.88 mAs; (6) 120 kV without filter, 1.92 mAs; (7) 120 kV with 0.2-mm filter, 3.6 mAs; (8) 140 kV without filter, 1.44 mAs. The detector-focus distance was 200 cm. Lung phantom images with different beam qualities were prepared by adjusting the milliampere-second value to maintain ESD identical (0.1 mGy) for all images. The ESD was obtained based on the previously described method [14]. The irradiation dose was measured in the free-in-air at a position of 177 cm which is the distance between the source and the

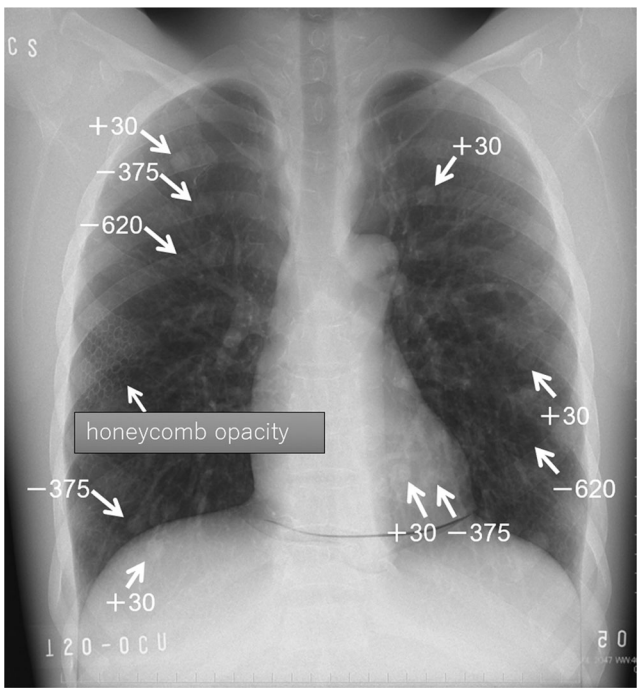

Fig. 1 Radiograph of realistic lung phantom. Arrows indicate simulated nodules and a simulated honeycomb opacity

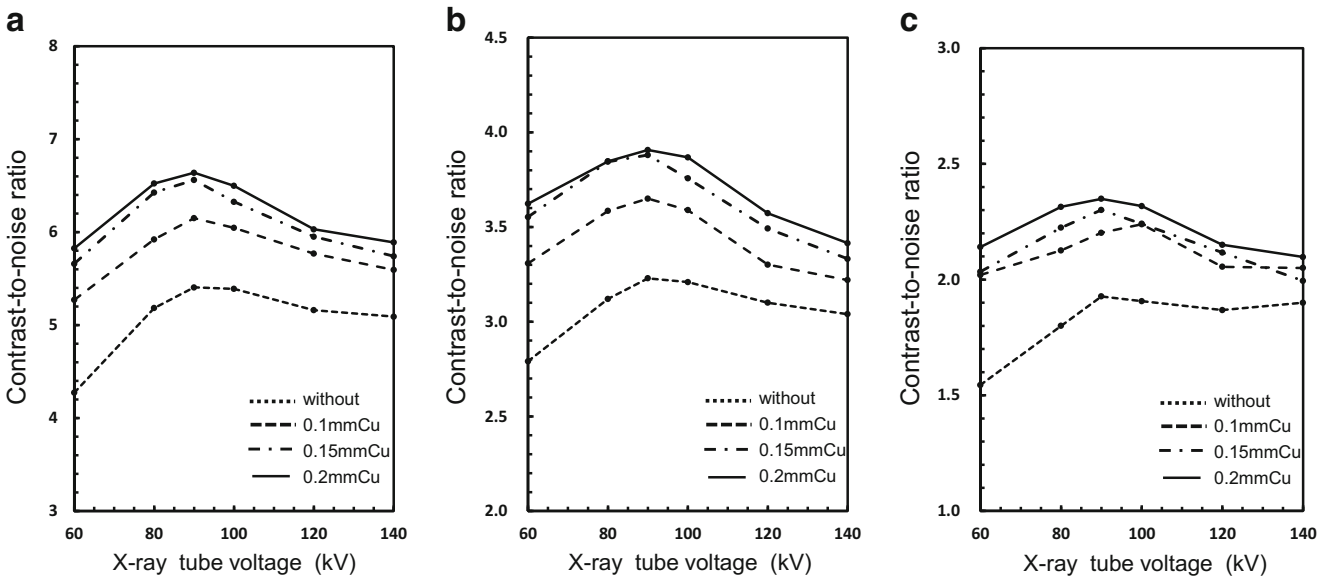

Fig. 2 Contrast-to-noise ratio (CNR) of simulated lung nodules according to using various X-ray tube voltage levels with or without copper using a 10-cm PMMA phantom under identical entrance skin dose (0.1 mGy). CT attenuation values of the nodules were + 30 HU (**a**), − 375 HU (**b**), and − 620 HU (**c**)

incident skin surface of the lung phantom. Dosimetry of various X-ray energies was performed using Radcal 1015 and 9060/10×5-60 ionization chamber dosimeter (Radcal Corporation). The ionization chamber dosimeters used were a tertiary standard, calibrated at a laboratory of the Japan Quality Assurance Organization. The values of the irradiation dose in roentgen or coulomb-per-kilogram obtained with the ion-chamber dosimeters were multiplied by backscatter coefficient, and the dose values were converted to the values of absorbed dose for soft tissue by using the ratio of mass energy absorption coefficient of "tissue, soft (ICRU-44)" to that of "air, dry (near sea level)" [15]. The milliampere-second was put manually. A 0.1-mm, a 0.15-mm, and a 0.2-mm copper filters backed by 1.0-mm aluminum were used for this study.

Qualitative assessment

Three chest radiologists independently evaluated the image quality of each simulated opacity and normal structure (vertebra and pulmonary vessels) using a 5-point scale. The traditional FPD image obtained at a tube voltage of 120 kV without copper filter was used as the standard (+ 2: the observed image clearly superior to the standard; + 1: the image slightly superior to the standard; 0: the image equal to the standard; − 1: the image slightly inferior to the standard; − 2: the image clearly inferior to the standard). The observers were blinded to the tube voltages and the usage of the copper filter. On the other hand, they were aware of the locations of the simulated opacities. There were three sets of image samples showing simulated opacities for the phantom lung. The scores of the three observers for a given set of images were totaled for each simulated opacity at each image and the averages per set were calculated.

Statistical method

The scores in image quality of each simulated opacity and normal structure were statistically compared using the Wilcoxon rank test. Bonferroni correction for post hoc pairwise analysis was performed to adjust for multiple comparisons. The level of significance was set at p values less than 0.05. Interobserver repeatability was assessed by intraclass correlation coefficients (ICC): ICC 0–0.2 indicates poor agreement; 0.3–0.4 indicates fair agreement; 0.5–0.6 indicates moderate agreement; 0.7–0.8 indicates strong agreement; and > 0.8 indicates excellent agreement [16]. All calculations were performed by using IBM SPSS Statistics, version 22.0 (IBM).

Results

Average scores for each simulated opacity and normal structure are summarized in Table 1. FPD images using 90-kV shot with 0.15- and 0.2-mm copper filters were superior to the traditional 120-kV shot without filter with respect to the visibility of vertebra, and nodules overlying right diaphragm and heart ($p < 0.05$) (Fig. 3). As for the visibility of pulmonary vessels, FPD image using 90-kV shot with 0.15-mm copper filters was also superior to the 120-kV shot without filter. Although FPD images using 100-kV shot with copper filters were superior to the traditional images with respect to the visibility of vertebra, there was no significant difference with respect to the visibility of the other simulated lung opacities. FPD images using 140-kV shot without filter were inferior to the traditional images with respect to the visibility of vertebra and pulmonary vessels. The ICC showed an excellent interobserver agreement in the qualitative

Table 1 Summary of average image scores for simulated opacities

Simulated opacity and normal structure (attenuation value)	Tube voltage and copper filter						
	90-kV 0.2-mm Cu	90-kV 0.15-mm Cu	100-kV 0.2-mm Cu	100-kV 0.1-mm Cu	100-kV Cu(−)	120-kV 0.2-mm Cu	140-kV Cu(−)
Nodule overlying 1st rib in rt ULF (+30)	0.11	0.11	0.00	0.00	−0.11	0.00	0.00
Nodule overlying 5th rib in rt ULF (−375)	0.11	0.11	0.00	0.11	0.00	0.00	0.00
Nodule overlying 6th rib in rt ULF (−620)	0.00	0.22	0.11	0.00	0.00	0.00	−0.11
Nodule above the diaphragm in rt LLF (−375)	0.00	0.00	0.00	0.00	−0.11	0.11	−0.33
Nodule overlying rt diaphragm (+30)	1.00*	1.00*	0.00	0.00	0.33	0.00	0.00
Nodule overlying 5th rib in lt ULF (+30)	0.11	0.22	0.11	0.00	0.00	0.00	0.00
Nodule in lt MLF (+30)	0.22	0.00	0.00	0.11	−0.11	0.11	−0.22
Nodule in lt LLF (−620)	0.11	0.00	0.00	0.00	0.00	0.00	0.00
Nodule overlying heart (−375)	0.33	0.11	0.11	0.11	0.00	0.00	−0.22
Nodule overlying heart (+30)	1.00*	1.00*	0.67	0.44	0.00	0.00	0.00
Honeycomb	0.00	0.00	0.00	0.00	0.00	0.11	−0.22
Pulmonary vessels	0.67	1.00*	0.00	0.44	0.00	0.00	−0.44
Vertebra	1.00*	1.00*	0.33	1.00*	0.00	0.33	−1.00*

rt, right; *lt*, left; *ULF*, upper lung field; *MLF*, middle lung field; *LLF*, lower lung field

*$p < 0.05$

measurements of the target nodules and structures (ICC = 0.831). Figures 4 and 5 show representative FPD images of realistic lung phantom showing nodule overlying right diaphragm and vertebra using 90-kV shot with copper filter and using traditional 120-kV shot without filter.

There was no significant difference with respect to the visibility of all other simulated lung opacities (lung nodules except for overlying diaphragm/heart and honeycomb opacity) between each tube voltage level with/without copper filter and the traditional 120-kV shot without filter.

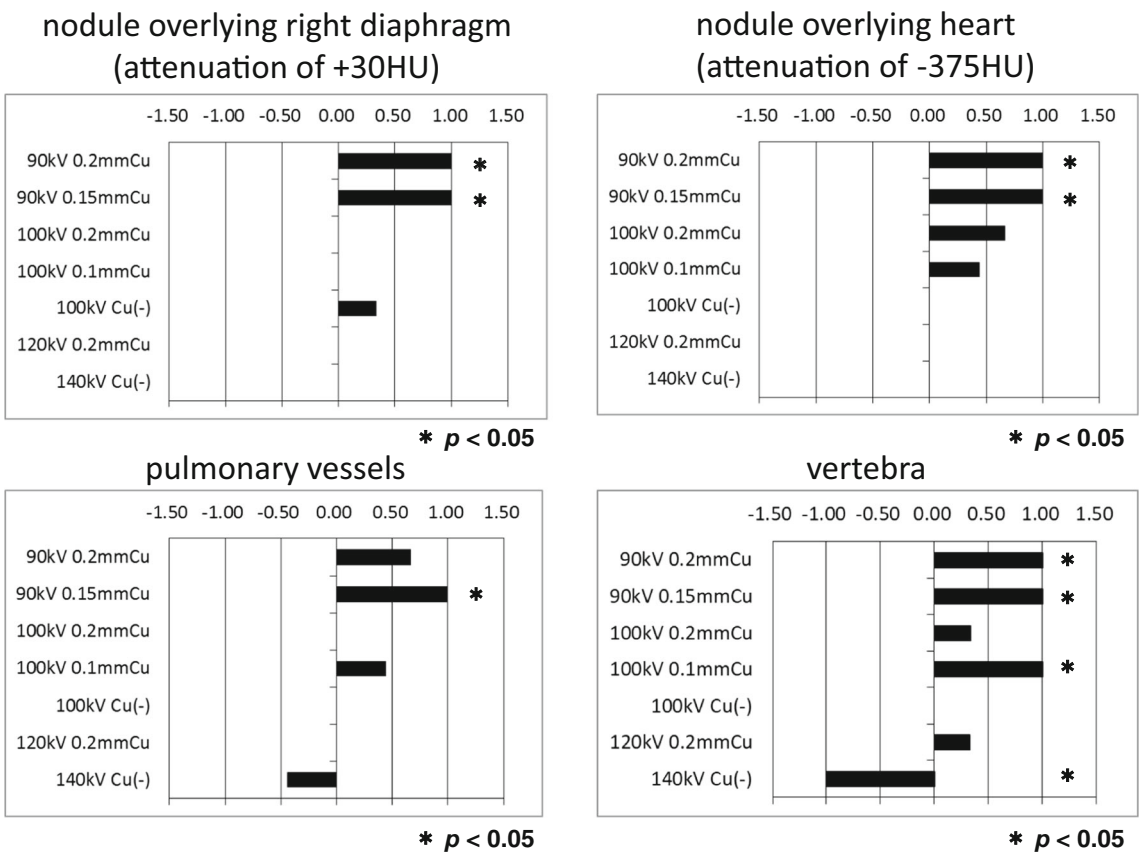

Fig. 3 Average scores for representative simulated opacities and normal structures. Wilcoxon rank test with Bonferroni correction was applied

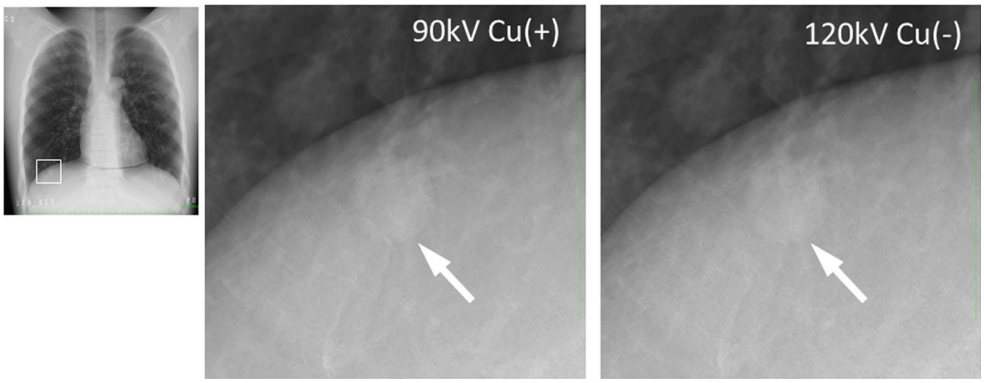

Fig. 4 FPD images of realistic lung phantom showing nodule overlying right diaphragm. Nodule contour on FPD image (arrows) using 90-kV shot with copper filter is clearer than that on FPD image using traditional 120-kV shot without filter

Discussion

Chest radiography is a proven and useful procedure for evaluating the airways, lungs, pulmonary vessels, and mediastinum [3]. Dobbins et al assessed the optimization of chest X-ray spectrum for a cesium iodide-amorphous silicon FPD, and they regarded 120 kV as the optimal beam quality when considering patient exposure using ESD and the ratio of tissue contrast to bone contrast simultaneously [17]. Although ESD inevitably increases with lower kilovoltage, the copper filter improves the increase trend of ESD remarkably [18, 19]. Previous investigators have suggested that image quality in high absorption areas, such as nodule contrast relative to the contrast of bone, improved with increasing tube voltage [10, 17]. However, there was no significant difference with respect to the visibility of lung nodules overlying ribs between low tube voltage level with copper filter and the traditional 120-kV shot without filter in this study.

Our study showed that FPD images using 90-kV shot with 0.15- and 0.2-mm copper filters showed the best visibility of simulated nodules and normal structures among FPD image valuables, when comparing with the FPD images using the traditional 120-kV shot. This result concurs with the quantitative result based on the CNR assessment of the simulated nodule using a PMMA plates phantom. The CNRs of the + 30 HU, − 375 HU, and – 620 HU nodules using 90–100-kV shot with copper filter were significantly higher than those using traditional 120–140-kV shot without filter (Fig. 2). Consequently, both in quality and in quantity, we believe that 90-kV shot with copper filter is suitable for chest FPD images. Considering the tube loading in clinical application and exposure time, 90-kV shot with a thinner copper filter might be recommended for chest FPD images.

On the basis of physical properties, lowering the kilovoltage increases absorption by the bones such as ribs, and one would suspect that the underlying lung parenchyma would be obscured as a consequence. However, this effect is much less apparent in DR than in conventional screen film radiography. Data processing in DR is chosen to achieve a compression of the dynamic range, which results in a global decrease in large density differences [6]. In addition, our previous experimental study showed that the effective energy of 90-kV shot with copper filter was slightly higher than 36 keV, which is a favorable k-absorption edge of cesium. This could result in improvement of energy conversion efficacy and noise characteristics. Data processing and the change of the effective energy by using copper filter might explain the superiority in the visibility of vertebra, pulmonary vessels, and nodules overlying the right diaphragm and heart on the FPD images using the lower kilovoltage shot with copper filter.

We compared the image quality of FPD images by using a lung phantom on the condition that the ESD was identical. Implementation of the optimum spectrum in clinical chest FPD imaging might permit a reduction in patient dose with image quality comparable with the current chest radiography standard. Further clinical research considering both image quality and dose would be performed.

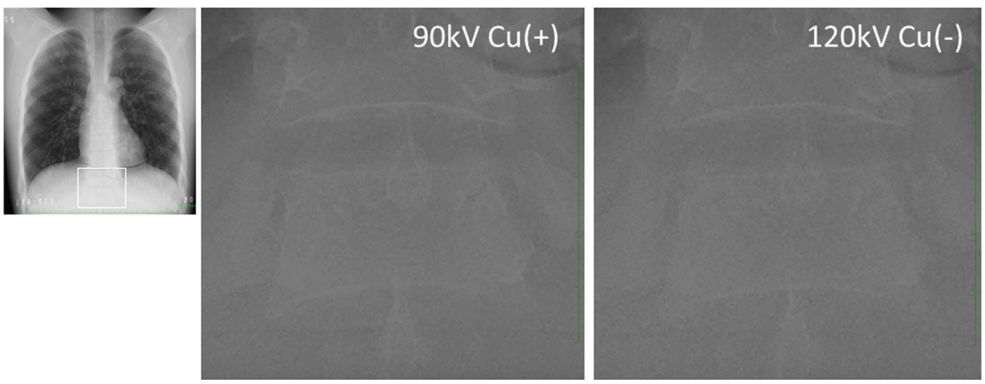

Fig. 5 FPD images of realistic lung phantom showing vertebra. Vertebra contour on FPD image using 90-kV shot with copper filter is clearer than that on FPD image using traditional 120-kV shot without filter

Our study had several limitations. First, we analyzed the limited opacity (nodule, honeycomb) and normal structure (vertebra, pulmonary vessels). In a clinical situation, additional abnormalities such as pleural effusion and mediastinal/chest wall abnormalities would need to be addressed. Second, the realistic phantom did not possess all of the characteristics of a human target and might not adequately account for measurement distortion induced by physical properties of living tissues. Third, we compared the image quality of FPD images on the condition that the ESD was identical, but calculation of the effective dose is regarded as a more appropriate indicator of the risk associated with different kilovoltage settings than ESD [18]. The effective dose equivalent remains relatively constant with lower kilovoltage. We therefore might have overestimated the patient risk and underestimated the effect on improvement of image quality. Finally, the phantom consisted of an accurate life-size anatomical model based on an Eastern male thorax. Further analyses using in vivo data of various physiques needs to be investigated to confirm optimal FPD beam in a clinical situation.

In conclusion, our phantom study demonstrated that image quality of chest FPD images using 90 kV with filter is superior to that using traditional beam when dose is identical. Further clinical study dealing with chest FPD beam optimization would be warranted.

Funding The authors state that this work has not received any funding.

Compliance with ethical standards

Guarantor The scientific guarantor of this publication is Takatoshi Aoki.

Conflict of interest The authors of this manuscript declare no relationships with any companies whose products or services may be related to the subject matter of the article.

Statistics and biometry No complex statistical methods were necessary for this paper.

Informed consent Informed consent was waived because of phantom study.

Ethical approval Institutional Review Board approval was not required because of phantom study.

Methodology
• experimental
• performed at one institution

References

1. Körner M, Weber CH, Wirth S, Pfeifer KJ, Reiser MF, Treitl M (2007) Advances in digital radiography: physical principles and system overview. Radiographics 27:675–686
2. Vaño E, Fernández JM, Ten JI et al (2007) Transition from screen-film to digital radiography: evolution of patients radiation doses at projection radiography. Radiology 243:461–466
3. American College of Radiology (2014) ACR–SPR–STR practice parameter for the performance of chest radiography. Available via https://www.acr.org/-/media/ACR/Files/Practice-Parameters/ChestRad.pdf. Accessed 12 Oct 2017
4. Asada Y, Suzuki S, Kobayashi K et al (2012) Summary of results of the patients exposures in diagnostic radiography in 2011 questionnaire-focus on radiographic conditions. Nihon Hoshasen Gijutsu Gakkai Zasshi 68:1261–1268
5. Matsunaga Y, Kawaguchi A, Kobayashi K et al (2017) Patients exposure during plain radiography and mammography in Japan in 1974-2014. Radiat Prot Dosim 176:347–353
6. Oda N, Nakata H, Murakami S, Terada K, Nakamura K, Yoshida A (1996) Optimal beam quality for chest computed radiography. Invest Radiol 31:126–131
7. Launders JH, Cowen AR, Bury RF, Hawkridge P (1998) A case study into the effect of radiographic factors on image quality and dose for a selenium based digital chest radiography system. Radiat Prot Dosim 80:279–282
8. Chotas HG, Floyd CE Jr, Dobbins JT 3rd, Ravin CE (1993) Digital chest radiography with photostimulable storage phosphors: signal-to-noise ratio as a function of kilovoltage with matched exposure risk. Radiology 186:395–398
9. Uffmann M, Neitzel U, Prokop M et al (2005) Flat-panel-detector chest radiography: effect of tube voltage on image quality. Radiology 235:642–650
10. Ullman G, Sandborg M, Dance DR, Hunt RA, Alm Carlsson G (2006) Towards optimization in digital chest radiography using Monte Carlo modelling. Phys Med Biol 51:2729–2743
11. Willemink MJ, Leiner T, Budde RP et al (2012) Systematic error in lung nodule volumetry: effect of iterative reconstruction versus filtered back projection at different CT parameters. AJR Am J Roentgenol 199:1241–1246
12. Xueqian X, Zhao Y, Snijder RA et al (2013) Sensitivity and accuracy of volumetry of pulmonary nodules on low-dose 16- and 64-row multi-detector CT: an anthropomorphic phantom study. Eur Radiol 23:139–147
13. Hashemi S, Mehrez H, Cobbold RS, Paul NS (2014) Optimal image reconstruction for detection and characterization of small pulmonary nodules during low-dose CT. Eur Radiol 24:1239–1250
14. Koyama S, Aoyama T, Oda N, Yamauchi-Kawaura C (2010) Radiation dose evaluation in tomosynthesis and C-arm cone-beam CT examinations with an anthropomorphic phantom. Med Phys 37:4298–4306
15. Hubbell JH, Seltzer SM (1995) "Tables of X-ray mass attenuation coefficients and mass energy-absorption coefficients 1 keV to 20 MeV for elements Z=1 to 92 and 48 additional substances of dosimetric interest," NISTIR 5632 National Institute of Standards and Technology, Gaithersdurg, MD
16. Landis JR, Koch GG (1977) The measurement of observer agreement for categorical data. Biometrics 33:159–174
17. Dobbins JT 3rd, Samei E, Chotas HG et al (2003) Chest radiography: optimization of x-ray spectrum for cesium iodide–amorphous silicon flat-panel detector. Radiology 226:221–230
18. ICRP (1991) 1990 Recommendations of the International Commission on Radiological Protection. ICRP Publication 60. Ann ICRP 21 1–3
19. Hamer OW, Sirlin CB, Strotzer M et al (2005) Chest radiography with a flat-panel detector: image quality with dose reduction after copper filtration. Radiology 237:691–700